Proceedings of the 10th International Workshop on Simulation for Energy, Sustainable Development & Environment (SESDE), 004
19th International Multidisciplinary Modeling & Simulation Multiconference

2724-0061 © 2022 The Authors.
doi: 10.46354/i3m.2022.sesde.004

2D Simulations of Water Treatment with Upscaled Capacitive Deionization

Johan Nordstrand*, Joydeep Dutta

Functional Materials, Applied Physics Department, School of Engineering Sciences, KTH Royal Institute of Technology, AlbaNova universitetscentrum 106 91 Stockholm, Sweden

*Corresponding author. Email address: johanno3@kth.se

Abstract

Clean water is a major global challenge. Meanwhile, capacitive deionization (CDI) is an emerging desalination technology that could help produce and reuse water. As the technology develops, the modeling of upscaled systems is becoming increasingly relevant. However, the inherent complexities in the CDI process have historically made such simulations unfeasible. In this work, we leverage the newly published electrolytic-capacitor (ECL) model to efficiently simulate parallel/serial flow modes in CDI stacks. The simulations are based on finite-element methods (FEM) that couple differential equations for describing local charging and ionic transport inside the device. The results show that both parallel and serial connections scale incredibly well with the system size. Still, parallel connections have the advantage of requiring lower pumping energy. Overall, we find that the relationship between adsorption capacity, flowrate, and compartment size is a good indicator of performance. In conclusion, the ELC model is promising for simulating upscaled CDI.

Keywords: Capacitive deionization; Desalination; Finite element; Modeling; Upscaling

1. Introduction

Global water scarcity has driven the United Nations (UN) to declare clean water as a key goal in agenda 2030 (goal 6) (Mekonnen & Hoekstra, 2016; UN, 2020; "WWAP (United Nations World Water Assessment Programme)/UN-Water," 2018). However, freshwater in rivers, lakes, and groundwater constitutes only 0.5 % of the water on earth (Kocera, 2014). Thus, sustainable solutions to this challenge will require us to not only reduce water consumption but also to produce more freshwater. Hence desalination (Alghoul et al., 2009; Fahmida & Sultana, 2018; Ghaffour et al., 2015; Greenlee et al., 2009; Kim et al., 2017; K. P. Lee et al., 2011; Mcginnis & Elimelech, 2007; Rommerskirchen, Ohs, et al., 2018; Sadhwani et al., 2005; Strathmann, 2010; Urtiaga et al., 2012). Capacitive deionization (CDI) is an emerging desalination technique that is well adapted to produce freshwater from brackish water and reuse wastewater (Anderson et al., 2010; Porada et al., 2013; Suss et al., 2015; Yu et al., 2016). Recent years have seen major developments in the technique, including stacks (Andres & Yoshihara, 2016; Gao et al., 2017; J. K. Lee et al., 2012; Mossad & Zou, 2013; Xing et al., 2019), pilot plants (Tan et al., 2018), and startup companies (Kunjali, 2022).

CDI is based on electrochemical desalination. It uses supercapacitor cells with porous electrodes and non-conducting spacers. During desalination, water flows through the device while an external potential drives the salt ions to adsorb on the electrodes. Even for just a single cell, the internal charging dynamics can be complicated because the process depends heavily on

the material (Gao et al., 2014; Guyes et al., 2017; Laxman et al., 2019; Li et al., 2010; Mutha et al., 2018; Nordstrand, Toledo-Carrillo, et al., 2022; Qin et al., 2021; Qu et al., 2018; Rommerskirchen, Linnartz, et al., 2018; Santos et al., 2018; Singh et al., 2020; Suss et al., 2013; Toledo-Carrillo et al., 2020; Vafakhah et al., 2019; G. Wang et al., 2011; Xu et al., 2018; Zhao et al., 2020), operational (Biesheuvel, 2015; Biesheuvel et al., 2014; Demirer et al., 2013; Hassanvand et al., 2018; Nordstrand & Dutta, 2020b, 2020c; C. Wang et al., 2015; Zhang et al., 2019), and structural conditions (Nordstrand & Dutta, 2020d; Tang et al., 2019). On top of this, simulating pilot-plant scales introduces even more complexity.

So, how could a pilot plant be modeled? Finite element methods (FEM) are powerful for simulating internal dynamics. The complicated part is the theory. Traditional methods in CDI, such as the modified Donnan (mD) model (Biesheuvel, Fu, et al., 2011; Guyes et al., 2017; Hemmatifar et al., 2015; Porada et al., 2013; Suss et al., 2014, 2015), have been powerful for simulating the single-cell system in 0D (Biesheuvel et al., 2009; Nordstrand et al., 2019; Nordstrand & Dutta, 2019, 2021b; Ramachandran et al., 2018), 1D (Biesheuvel, Fu, et al., 2011; Biesheuvel, Zhao, et al., 2011; Biesheuvel & Bazant, 2010; Guyes et al., 2017; Mutha et al., 2018; Perez et al., 2013; Suss et al., 2012, 2014), and ideal 2D (Hemmatifar et al., 2015; Nordstrand & Dutta, 2021a). However, the authors report that such 2D simulations can be unsteady (Hemmatifar et al., 2015). Others have tried using decoupled modeling to be able to simulate higher dimensions (Xiaobing et al., 2021), generalized operations (Nordstrand & Dutta, 2021a), and larger (2-cell) stacks (Nordstrand & Dutta, 2021c). Still, fully coupled simulations remain a challenge and studies often simulate specific aspects when it comes to upscaling (Nordstrand & Dutta, 2020d).

In this work, we present an extended model and simulate different configurations of large stacks of CDI cells in 2D. This is possible based on a recently published model, named the electrolytic-capacitor (ELC) model (Nordstrand, Zuili, et al., 2022). The model has, so far, only been used in single-cell simulations. However, its theory-base stabilizes simulations, while its generalized implementation supports complex device structures. This is ideal for upscaled simulations. Aside from presenting the model, this work seeks to answer the specific question: is it better to use serial or parallel connections with cells in a large stack?

2. Methods

To compare the stack connections, we need to know what the geometry looks like. A single device consists of two electrodes separated by a spacer region (Figure 1). The water flows in the spacer region. Meanwhile, external voltages are applied via current collectors to the outside of the electrodes. This means the salt ions in the spacer channel will diffuse into the electrodes and adsorb.

For the upscaling, the connected geometry is also important. Figure 1 shows the stack configurations with either parallel or serial connections. In the parallel case, the spacer is porous while the pipes are open. This makes the flow pressure-driven while going through the cells, meaning the flow passing through all the cells will be identical. In the serial case, the flow pathway is five times longer, but the velocity is also five times higher (for the same volumetric flowrate).

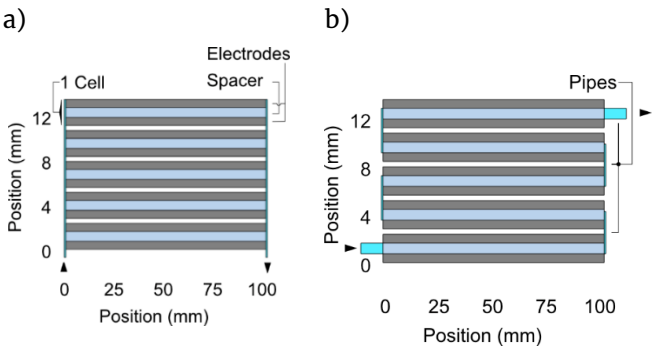

Figure 1. The device structures that are considered in this work. Both are stacks containing 5 CDI cells. Each cell comprises two electrodes and a separating spacer. The water flow follows the arrows; it enters on the left and passes the stack before exiting on the right. (a) Parallel flow. The water distributes amongst the cells before converging in the output stream. (b) Serial flow. The same flow passes all cells in a series.

This work presents simulations using the ELC model as derived in our Ref. (Nordstrand, Zuili, et al., 2022). That work only uses it to simulate a single-cell device, and we here extend the geometry to stacks of CDI cells. The model uses finite-element methods (FEM) to locally solve the desalination process. The key components include water flow generating convection, currents in the electrode generating adsorption, and ionic transport leading to clean output water.

Briefly, the external potential in the model generates a potential ϕ_s in the electrode (subscript s for solid). When the potential in the electrode rises relative to the liquid potential ϕ_l, this leads to double-layer charging (Eq. 1). Similar to a normal capacitance, the local double-layer current source at the electrode i_{dl} is equal to the local capacitance C_{dl} times the derivative of the potential difference. This current then passes the liquid and the relationship between the liquid potential ϕ_l and the current $\boldsymbol{i_l}$ follows Ohm's law with a concentration-dependent conductivity σ_l (Eq. 2). The charging leads to adsorption and the charge-efficiency parameter ν determines the relationship between ideal charging and adsorption rate R_i (Eq. 3). The overall transport of ions then depends on convection, diffusion, and electromigration. For the overall salt transport, only convection and diffusion matter here because the KCl solution is charge-neutral (Eq. 4). More details can be

found in Ref. (Nordstrand, Zuili, et al., 2022).

$$i_{dl} = C_{dl}\frac{\partial(\phi_s - \phi_l)}{\partial t} \quad (1)$$

$$\boldsymbol{i_l} = -\sigma_l \nabla \phi_l \quad (2)$$

$$R_i = -\frac{\nu i_{v,dl}}{nF} \quad (3)$$

$$\frac{\partial c_i}{\partial t} + \nabla \cdot (-D_i \nabla c_i) + \boldsymbol{u} \cdot \nabla c_i = R_i \quad (4)$$

Unless otherwise noted, the simulated voltage is 0.6 V across each cell, the inlet concentration is 20 mM KCl, and the flowrate is 0.42 mL/min times the number of cells.

The model implementation is in COMSOL Multiphysics. Thus, the Brinkman Equations interfaces calculate the fluid flow. The Secondary Current distribution calculates the charging. The Transport of Diluted Species interfaces calculates ionic transport. Also, the Event interface handles switching between desalination and regeneration modes during the operation.

3. Results and Discussion

3.1. The Behavior of a Single Cell

The CDI device fundamentally behaves like a capacitor (Nordstrand & Dutta, 2020a; Nordstrand & Joydeep, 2020), but charging it serves to remove ions rather than store energy. Thus, **Figure 2**a shows that the charging characteristics are similar to an RC circuit. That is, the charging increases exponentially with time, and a higher voltage raises the maximum storage. In fact, previous work has suggested that contact resistance is the biggest source of resistance in the circuit (Dykstra et al., 2016). However, a deviation can be seen for the highest voltage (1 V). Here, the strong adsorption makes the spacer channel ion starved, meaning the conductivity is so low that it slows the entire charging process.

Three fitting parameters have been extracted from the experiment data to tune the model. These are important to note because they represent the main degrees of freedom in the system. The first parameter is the overall circuit resistance (mainly from contacts), the second is the specific capacitance of the material, and the third is the charge efficiency (fraction of current leading to adsorption).

Aside from charging characteristics, another key aspect of the system is that the transport inside the device delays the desalination output compared to the internal charging (**Figure 2**b). On one hand, it takes time for the ions to diffuse through the porous electrodes. On the other hand, it takes time for the convective flow to push clean water out of the device. Here, again, we can see that the ion-starved conditions at 1 V are the most difficult to simulate accurately.

Looking at the inside of the device, these transport phenomena lead to a concentration wavefront inside the electrodes (**Figure 2**c). First, the charging removes most of the ions inside the electrode on the top and bottom. Then, the ions diffuse in and deplete the spacer channel. But the water with new ions enters at the inlet, so the areas of the electrode close to the inlet tend to get replenished fast. Having low concentration can cause starvation that slows the charging process, as demonstrated in the data for the operation at 1 V. For the upscaled system, this starvation effect leads to an interesting question: What configuration gives the most uniform internal removal?

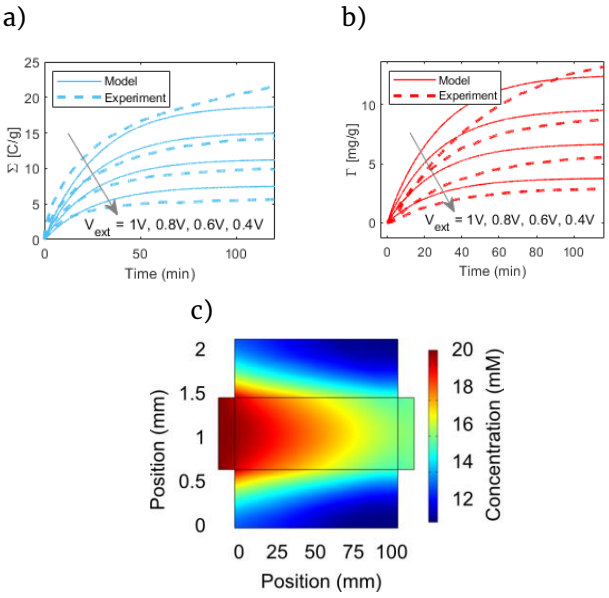

Figure 2. Performance of the single-cell device. The experiment data and simulations are the same as in the model publication in Ref. (Nordstrand, Zuili, et al., 2022) (although the graphics are new). (a) The specific charge (C per g electrode) during the charging. (b) The specific ion removal (mg KCl per g electrode) during the charging process. (c) The internal concentration after 20 minutes of operation. The water enters from the left, travels through the central spacer region, and exits on the right. The top and bottom regions are the electrodes.

3.2. Serial Connection

A natural way to build a larger CDI module is to make a stack with multiple cells and make the outlet of one cell become the inlet of the next cell, in a long series. However, this could potentially lead to issues. The distance between the inlet and output is now much longer than in the single-cell case, so the removal differences might get larger. To make the situation

comparable, we will use a flowrate that is proportional to the number of cells in the stack and calculate the performance per cell in the stack.

Interestingly, the behavior per cell is almost the same for the 5-cell serial stack (**Figure 3**a). Both the energy consumption and removal are highly similar. The output concentration also follows a similar trend. In the single-cell case, we could see a removal imbalance wherein the concentration was lower at the back end of the electrode near the outlet. Here, the same imbalance exists both between cells and within cells. That is, there are lower concentrations near the outlet corners that the inlet concentration within a device. There is also a lower concentration in the last cells compared to the first cells. Overall, we can thus conclude that the serial stack scales well in terms of behavior. This is an interesting result because if depletion could be an issue for a single cell, we might expect the last cell in a stack to have much worse issues with depletion. But that effect seems to be entirely compensated for with the proportionally higher flowrate.

Another likely explanation for the results is that the resistance in the circuit is mainly external (between electrodes and current collectors) as mentioned earlier (Dykstra et al., 2016). This means the electrodes usually have the ability to charge faster internally than the external circuit allows. So, if small parts of the electrodes are locally starved, other parts will adsorb faster to reach the same overall charging rate. The starved regions will thus be replenished while other regions charge more, and the overall process will look similar.

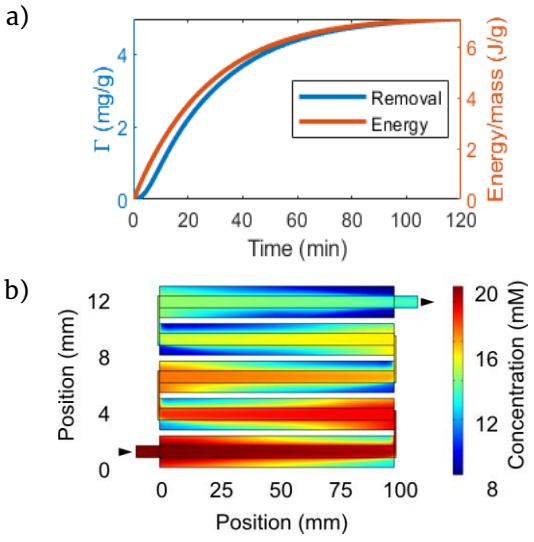

Figure 3. Performance of the serial connection. (a) The specific salt removal (mg KCl per g electrode) and specific charging energy (J per g electrode). (b) The internal concentration in the serial stack. The water enters from the lower left and traverses the spacers horizontally, one after another, before exiting on the upper right. Each cell in the stack has a separate voltage connection of 0.6 V.

3.3. Parallel Connections

Because the spacer is porous, the flowing water requires pumping power to be able to pass the spacers at a required velocity. This becomes an issue in the serial system. In an N-cell stack, the flow pathway is N times as long and the required velocity is N times as high. This gives an N^2 scaling of the pumping power compared to the single-cell system. Just having N separate devices should only scale the power with N, so N^2 is not ideal. One way to mitigate this is by using parallel connections.

In the parallel connection, the cells have a common inlet pipe but are otherwise separate. This should give ideal scaling from the single-cell device. The results for the charging energy and ion removal confirm this (**Figure 4**a). It is also interesting to note that the performance is almost like the serial case (**Figure 4**a). Thus, we conclude that the systems are largely equivalent except for the pumping energy.

Here, we have not discussed which upscaled system is more practical to build, although we recognize that practical issues should play a role in real pilot plants. Rather, the point is the get a solid understanding of what the operations look like, to illustrate how the systems should behave when built.

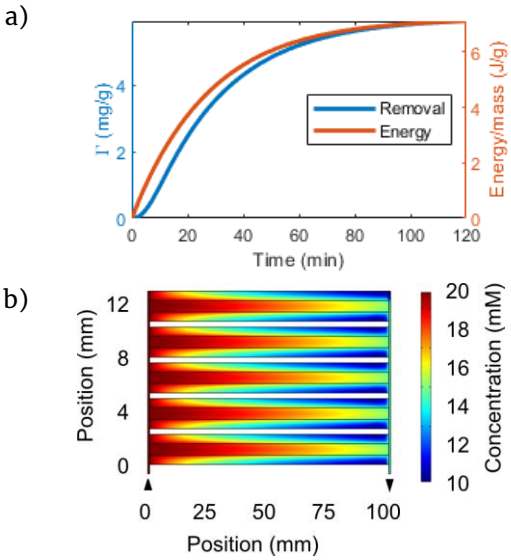

Figure 4. Performance of the parallel connection. (a) The specific salt removal (mg KCl per g electrode) and specific charging energy (J per g electrode). (b) The internal concentration in the parallel stack. The water enters from the lower left and traverses the spacers horizontally before exiting on the lower right. Each cell in the stack has a separate voltage connection of 0.6 V.

3.4. Even Bigger

As a final note, we would like to mention that the number of cells N in the stack is a parameter input in the model. This makes it straightforward to simulate stacks of any size. For a single cell or a small stack, a laptop is enough to complete the simulations. However, we have also checked the model for stacks with over 100 cells using cluster resources.

4. Conclusions

Upscaling is essential for making desalination by CDI commercially viable. However, it is challenging for modeling. Here, we have demonstrated that it is possible to simulate a large CDI stack using a model with full spatial coupling (the ELC model). This is significant because it demonstrates that researchers now have a set tool to use for investigating further variations in upscaled structures.

We also investigate serial and parallel flow connections in CDI stacks. The results show that both have excellent scaling. That is, the charging energy and ion removal are almost the same per cell as in the single-cell device. However, the serial stack requires more energy for pumping because of the longer pathways that the water flow must traverse. Overall, we have learned that the macroscopic relationship between adsorption capacity, flowrate, and internal volume is a good indicator of performance for both connection types.

5. Funding

The authors would like to thank the Swedish research council (Diary No. 2018-05387) and J. Gust. Richert foundation (Diary No. 2020-00584) for funding the work, and the SNIC PDC supercomputing center (PDC-2021-56) for providing computing resources.

6. References

Alghoul, M. A., Poovanaesvaran, P., Sopian, K., & Sulaiman, M. Y. (2009). Review of brackish water reverse osmosis (BWRO) system designs. *Renewable and Sustainable Energy Reviews*, *13*, 2661–2667. https://doi.org/10.1016/j.rser.2009.03.013

Anderson, M. A., Cudero, A. L., & Palma, J. (2010). Capacitive deionization as an electrochemical means of saving energy and delivering clean water. Comparison to present desalination practices: Will it compete? *Electrochimica Acta*, *55*(12), 3845–3856. https://doi.org/10.1016/j.electacta.2010.02.012

Andres, G. L., & Yoshihara, Y. (2016). A capacitive deionization system with high energy recovery and effective re-use. *Energy*, *103*, 605–617. https://doi.org/10.1016/j.energy.2016.03.021

Biesheuvel, P. M. (2015). Activated carbon is an electron-conducting amphoteric ion adsorbent. *ArXiv*. http://arxiv.org/abs/1509.06354

Biesheuvel, P. M., & Bazant, M. Z. (2010). Nonlinear dynamics of capacitive charging and desalination by porous electrodes. *Physical Review E - Statistical, Nonlinear, and Soft Matter Physics*, *81*(3), 1–12. https://doi.org/10.1103/PhysRevE.81.031502

Biesheuvel, P. M., Fu, Y., & Bazant, M. Z. (2011). Diffuse charge and Faradaic reactions in porous electrodes. *Physical Review E*, *83*(6). https://doi.org/10.1103/PhysRevE.83.061507

Biesheuvel, P. M., Limpt, B. Van, & Wal, a Van Der. (2009). Dynamic Adsorption / Desorption Process Model for Capacitive Deionization. *Journal of Physical Chemistry C*, *113*(March), 5636–5640. https://doi.org/10.1021/jp809644s

Biesheuvel, P. M., Porada, S., Levi, M., & Bazant, M. Z. (2014). Attractive forces in microporous carbon electrodes for capacitive deionization. *Journal of Solid State Electrochemistry*, *18*(5), 1365–1376. https://doi.org/10.1007/s10008-014-2383-5

Biesheuvel, P. M., Zhao, R., Porada, S., & van der Wal, A. (2011). Theory of membrane capacitive deionization including the effect of the electrode pore space. In *Journal of Colloid and Interface Science* (Vol. 360, Issue 1, pp. 239–248). https://doi.org/10.1016/j.jcis.2011.04.049

Demirer, O. N., Naylor, R. M., Rios Perez, C. A., Wilkes, E., & Hidrovo, C. (2013). Energetic performance optimization of a capacitive deionization system operating with transient cycles and brackish water. *Desalination*, *314*, 130–138. https://doi.org/10.1016/j.desal.2013.01.014

Dykstra, J. E., Zhao, R., Biesheuvel, P. M., & Wal, A. Van Der. (2016). Resistance identification and rational process design in Capacitive Deionization. *Water Research*, *88*, 358–370. https://doi.org/10.1016/j.watres.2015.10.006

Fahmida, P., & Sultana, A. (2018). Desalination Technologies for Developing Countries : A Review. *Journal of Scientific Research*, *10*(January), 77–97. https://doi.org/10.3329/jsr.v10i1.33179

Gao, X., Omosebi, A., Holubowitch, N., Landon, J., & Liu, K. (2017). Capacitive Deionization Using Alternating Polarization: Effect of Surface Charge on Salt Removal. *Electrochimica Acta*, *233*, 249–255. https://doi.org/10.1016/j.electacta.2017.03.021

Gao, X., Omosebi, A., Landon, J., & Liu, K. (2014). Enhancement of charge efficiency for a capacitive deionization cell using carbon xerogel with modified potential of zero charge. *Electrochemistry Communications*, *39*, 22–25. https://doi.org/10.1016/j.elecom.2013.12.004

Ghaffour, N., Missimer, T. M., & Amy, G. L. (2015). Technical review and evaluation of the economics of water desalination : Current and

future challenges for better water supply sustainability. *DES*, *309*(2013), 197–207. https://doi.org/10.1016/j.desal.2012.10.015

Greenlee, L. F., Lawler, D. F., Freeman, B. D., Marrot, B., Moulin, P., & Ce, P. (2009). Reverse osmosis desalination : Water sources , technology , and today ' s challenges. *Water Research*, *43*(9), 2317–2348. https://doi.org/10.1016/j.watres.2009.03.010

Guyes, E. N., Shocron, A. N., Simanovski, A., Biesheuvel, P. M., & Suss, M. E. (2017). A one-dimensional model for water desalination by flow-through electrode capacitive deionization. *Desalination*, *415*, 8–13. https://doi.org/10.1016/j.desal.2017.03.013

Hassanvand, A., Chen, G. Q., Webley, P. A., & Kentish, S. E. (2018). A comparison of multicomponent electrosorption in capacitive deionization and membrane capacitive deionization. *Water Research*, *131*, 100–109. https://doi.org/10.1016/j.watres.2017.12.015

Hemmatifar, A., Stadermann, M., & Santiago, J. G. (2015). Two-Dimensional Porous Electrode Model for Capacitive Deionization. *Journal of Physical Chemistry C*, *119*(44), 24681–24694. https://doi.org/10.1021/acs.jpcc.5b05847

Kim, T., Gorski, C. A., & Logan, B. E. (2017). Low Energy Desalination Using Battery Electrode Deionization [Rapid-communication]. *Environmental Science and Technology Letters*, *4*(10), 444–449. https://doi.org/10.1021/acs.estlett.7b00392

Kocera, J. (2014). *Desalination - Water to water*. John Wiley & Sons.

Kunjali, K. L. (2022). *Stockholm Water*. https://stockholmwater.com/

Laxman, K., Husain, A., Nasser, A., Al, M., & Dutta, J. (2019). Tailoring the pressure drop and fluid distribution of a capacitive deionization device. *Desalination*, *449*(July 2018), 111–117. https://doi.org/10.1016/j.desal.2018.10.021

Lee, J. K., Kim, Y. E., Kim, J., Chung, S., Ji, D., & Lee, J. (2012). Comparable mono and bipolar connection of capacitive deionization stack in NaCl treatment. *Journal of Industrial and Engineering Chemistry*, *18*(2), 763–766. https://doi.org/10.1016/j.jiec.2011.11.119

Lee, K. P., Arnot, T. C., & Mattia, D. (2011). A review of reverse osmosis membrane materials for desalination — Development to date and future potential. *Journal of Membrane Science*, *370*(1–2), 1–22. https://doi.org/10.1016/j.memsci.2010.12.036

Li, H., Zou, L., Pan, L., & Sun, Z. (2010). Using graphene nano-flakes as electrodes to remove ferric ions by capacitive deionization. *Separation and Purification Technology*, *75*(1), 8–14. https://doi.org/10.1016/j.seppur.2010.07.003

Mcginnis, R. L., & Elimelech, M. (2007). Energy requirements of ammonia – carbon dioxide forward osmosis desalination. *Desalination*, *207*, 370–382. https://doi.org/10.1016/j.desal.2006.08.012

Mekonnen, M. M., & Hoekstra, A. Y. (2016). Four billion people facing severe water scarcity. *Science Advances*, *2*(February), 1–7. https://doi.org/DOI: 10.1126/sciadv.1500323

Mossad, M., & Zou, L. (2013). Evaluation of the salt removal efficiency of capacitive deionisation: Kinetics, isotherms and thermodynamics. *Chemical Engineering Journal*, *223*, 704–713. https://doi.org/10.1016/j.cej.2013.03.058

Mutha, H. K., Cho, H. J., Hashempour, M., Wardle, B. L., Thompson, C. V., & Wang, E. N. (2018). Salt rejection in flow-between capacitive deionization devices. *Desalination*, *437*(January), 154–163. https://doi.org/10.1016/j.desal.2018.03.008

Nordstrand, J., & Dutta, J. (2019). Dynamic Langmuir Model: A Simpler Approach to Modeling Capacitive Deionization. *Journal of Physical Chemistry C*, *123*(26), 16479–16485. https://doi.org/10.1021/acs.jpcc.9b04198

Nordstrand, J., & Dutta, J. (2020a). Basis and Prospects of Combining Electroadsorption Modeling Approaches for Capacitive Deionization. *Physics*, *2*(2), 309–324. https://doi.org/10.3390/physics2020016

Nordstrand, J., & Dutta, J. (2020b). Predicting and Enhancing the Ion Selectivity in Multi-ion Capacitive Deionization. *Langmuir*, *36*(29), 8476–8484. https://doi.org/10.1021/acs.langmuir.0c00982

Nordstrand, J., & Dutta, J. (2020c). Simplified Prediction of Ion Removal in Capacitive Deionization of Multi-Ion Solutions. *Langmuir*, *36*(5), 1338–1344. https://doi.org/10.1021/acs.langmuir.9b03571

Nordstrand, J., & Dutta, J. (2020d). Design principles for enhanced up-scaling of flow-through capacitive deionization for water desalination. *Desalination*, *500*, 114842. https://doi.org/10.1016/j.desal.2020.114842

Nordstrand, J., & Dutta, J. (2021a). A new automated model brings stability to finite-element simulations of capacitive deionization. *Nano*

Select, *October*, 1–15. https://doi.org/10.1002/nano.202100270

Nordstrand, J., & Dutta, J. (2021b). Flexible Modeling and Control of Capacitive-deionization Processes through a Linear-state-space Dynamic-Langmuir Model. *Npj Clean Water*, *4*(5), 1–7. https://doi.org/10.1038/s41545-020-00094-y

Nordstrand, J., & Dutta, J. (2021c). Langmuir-Based Modeling Produces Steady Two- Dimensional Simulations of Capacitive Deionization via Relaxed Adsorption-Flow Coupling. *Langmuir*, 1–28. https://doi.org/https://doi.org/10.1021/acs.langmuir.1c02806

Nordstrand, J., & Joydeep, D. (2020). An Extended Randles Circuit and a Systematic Model-Development Approach for Capacitive Deionization. *Journal of the Electrochemical Society*. https://doi.org/Communicated 2020

Nordstrand, J., Laxman, K., Myint, M. T. Z., & Dutta, J. (2019). An Easy-to-Use Tool for Modeling the Dynamics of Capacitive Deionization. *Journal of Physical Chemistry A*, *123*(30), 6628–6634. https://doi.org/10.1021/acs.jpca.9b05503

Nordstrand, J., Toledo-Carrillo, E., Vafakhah, S., Guo, L., Yang, H. Y., Kloo, L., & Dutta, J. (2022). Ladder Mechanisms of Ion Transport in Prussian Blue Analogues. *ACS Applied Materials and Interfaces*, *14*(1), 1102–1113. https://doi.org/10.1021/acsami.1c20910

Nordstrand, J., Zuili, L., Alejandro, E., Carrillo, T., & Dutta, J. (2022). Predicting Capacitive Deionization Processes using an Electrolytic-Capacitor (ELC) Model. *Desalination*, *525*, 115493. https://doi.org/https://doi.org/10.1016/j.desal.2021.115493

Perez, C. A. R., Demirer, O. N., Clifton, R. L., Naylor, R. M., & Hidrovo, C. H. (2013). Macro Analysis of the Electro-Adsorption Process in Low Concentration NaCl Solutions for Water Desalination Applications. *Journal of the Electrochemical Society*, *160*(3), E13–E21. https://doi.org/10.1149/2.025303jes

Porada, S., Zhao, R., Van Der Wal, A., Presser, V., & Biesheuvel, P. M. (2013). Review on the science and technology of water desalination by capacitive deionization. *Progress in Materials Science*, *58*(8), 1388–1442. https://doi.org/10.1016/j.pmatsci.2013.03.005

Qin, M., Ren, W., Jiang, R., Li, Q., Yao, X., Wang, S., You, Y., & Mai, L. (2021). Highly Crystallized Prussian Blue with Enhanced Kinetics for Highly Efficient Sodium Storage. *ACS Applied Materials and Interfaces*, *13*(3), 3999–4007. https://doi.org/10.1021/acsami.0c20067

Qu, Y., Campbell, P. G., Hemmatifar, A., Knipe, J. M., Loeb, C. K., Reidy, J. J., Hubert, M. A., Stadermann, M., & Santiago, J. G. (2018). Charging and Transport Dynamics of a Flow-Through Electrode Capacitive Deionization System. *Journal of Physical Chemistry B*, *122*(1), 240–249. https://doi.org/10.1021/acs.jpcb.7b09168

Ramachandran, A., Hemmatifar, A., Hawks, S. A., Stadermann, M., & Santiago, J. G. (2018). Self similarities in desalination dynamics and performance using capacitive deionization. *Water Research*, *140*, 323–334. https://doi.org/10.1016/j.watres.2018.04.042

Rommerskirchen, A., Linnartz, C. J., Müller, D., Willenberg, L. K., & Wessling, M. (2018). Energy Recovery and Process Design in Continuous Flow - Electrode Capacitive Deionization Processes. *Sustainable Chemistry and Engineering*, *6*, 13007–13015. https://doi.org/10.1021/acssuschemeng.8b02466

Rommerskirchen, A., Ohs, B., Arturo, K., & Femmer, R. (2018). Modeling continuous flow-electrode capacitive deionization processes with ion-exchange membranes. *Journal of Membrane Science*, *546*(October 2017), 188–196. https://doi.org/10.1016/j.memsci.2017.10.026

Sadhwani, J. J., Veza, J. M., & Santana, C. (2005). Case studies on environmental impact of seawater desalination. *Desalination*, *185*(May), 1–8. https://doi.org/10.1016/j.desal.2005.02.072

Santos, C., Lado, J. J., Garcia-Quismondo, E., Soria, J., Palma, J., & Anderson, M. A. (2018). Maximizing Volumetric Removal Capacity in Capacitive Deionization by Adjusting Electrode Thickness and Charging Mode. *Journal of the Electrochemical Society*, *165*(7), 294–302. https://doi.org/10.1149/2.1011807jes

Singh, K., Qian, Z., Biesheuvel, P. M., Zuilhof, H., Porada, S., & de Smet, L. C. P. M. (2020). Nickel hexacyanoferrate electrodes for high mono/divalent ion-selectivity in capacitive deionization. *Desalination*, *481*, 114346. https://doi.org/10.1016/J.DESAL.2020.114346

Strathmann, H. (2010). Electrodialysis , a mature technology with a multitude of new applications. *DES*, *264*(3), 268–288. https://doi.org/10.1016/j.desal.2010.04.069

Suss, M. E., Baumann, T. F., Bourcier, W. L., Spadaccini, C. M., Rose, K. A., Santiago, J. G., & Stadermann, M. (2012). Capacitive desalination with flow-through electrodes. *Energy &*

Environmental Science, *5*(11), 9511. https://doi.org/10.1039/c2ee21498a

Suss, M. E., Baumann, T. F., Worsley, M. A., Rose, K. A., Jaramillo, T. F., Stadermann, M., & Santiago, J. G. (2013). Impedance-based study of capacitive porous carbon electrodes with hierarchical and bimodal porosity. *Journal of Power Sources*, *241*, 266–273. https://doi.org/10.1016/j.jpowsour.2013.03.178

Suss, M. E., Biesheuvel, P. M., Baumann, T. F., Stadermann, M., & Santiago, J. G. (2014). In situ spatially and temporally resolved measurements of salt concentration between charging porous electrodes for desalination by capacitive deionization. *Environmental Science and Technology*, *48*(3), 2008–2015. https://doi.org/10.1021/es403682n

Suss, M. E., Porada, S., Sun, X., Biesheuvel, P. M., Yoon, J., & Presser, V. (2015). Water desalination via capacitive deionization: what is it and what can we expect from it? *Energy Environ. Sci.*, *8*(8), 2296–2319. https://doi.org/10.1039/C5EE00519A

Tan, C., He, C., Tang, W., Kovalsky, P., Fletcher, J., & Waite, T. D. (2018). Integration of photovoltaic energy supply with membrane capacitive deionization (MCDI) for salt removal from brackish waters. *Water Research*, *147*, 276–286. https://doi.org/10.1016/j.watres.2018.09.056

Tang, W., Liang, J., He, D., Gong, J., Tang, L., Liu, Z., Wang, D., & Zeng, G. (2019). Various cell architectures of capacitive deionization: Recent advances and future trends. *Water Research*, *150*, 225–251. https://doi.org/10.1016/j.watres.2018.11.064

Toledo-Carrillo, E., Zhang, X., Laxman, K., & Dutta, J. (2020). Asymmetric electrode capacitive deionization for energy efficient desalination. *Electrochimica Acta*, *358*(13), 136939. https://doi.org/10.1016/j.electacta.2020.136939

UN. (2020). *Ensure availability and sustainable management of water and sanitation for all*. https://sdgs.un.org/goals/goal6

Urtiaga, A. M., Iba, R., & Ortiz, I. (2012). State of the art and review on the treatment technologies of water reverse osmosis concentrates. *Water Re*, *46*, 267–283. https://doi.org/10.1016/j.watres.2011.10.046

Vafakhah, S., Guo, L., Sriramulu, D., Huang, S., Saeedikhani, M., & Yang, H. Y. (2019). Efficient Sodium-Ion Intercalation into the Freestanding Prussian Blue/Graphene Aerogel Anode in a Hybrid Capacitive Deionization System. *ACS Applied Materials and Interfaces*, *11*(6), 5989–5998. https://doi.org/10.1021/acsami.8b18746

Wang, C., Song, H., Zhang, Q., Wang, B., & Li, A. (2015). Parameter optimization based on capacitive deionization for highly efficient desalination of domestic wastewater biotreated effluent and the fouled electrode regeneration. *Desalination*, *365*, 407–415. https://doi.org/10.1016/j.desal.2015.03.025

Wang, G., Ling, Y., Qian, F., Yang, X., Liu, X. X., & Li, Y. (2011). Enhanced capacitance in partially exfoliated multi-walled carbon nanotubes. *Journal of Power Sources*, *196*(11), 5209–5214. https://doi.org/10.1016/j.jpowsour.2011.02.019

WWAP (United Nations World Water Assessment Programme)/UN-Water. (2018). *The United Nations World Water Development Report 2018: Nature-Based Solutions for Water*.

Xiaobing, W., Jinqiu, L., Yang, L., Sen, L., Dong, L., Tingting, M., An, J., Yanshe, H., & Fengwei, G. (2021). Numerical Analysis of Capacitive Deionization Process Using Activated Carbon Electrodes. *Water, Air, and Soil Pollution*, *232*(9), 1–10. https://doi.org/10.1007/s11270-021-05320-y

Xing, W., Liang, J., Tang, W., Zeng, G., Wang, X., Li, X., Jiang, L., Luo, Y., Li, X., Tang, N., & Huang, M. (2019). Perchlorate removal from brackish water by capacitive deionization: Experimental and theoretical investigations. *Chemical Engineering Journal*, *361*(October 2018), 209–218. https://doi.org/10.1016/j.cej.2018.12.074

Xu, X., Li, J., Li, Y., Ni, B., Liu, X., & Pan, L. (2018). Selection of Carbon Electrode Materials. In Elsevier (Ed.), *Interface Science and Technology* (1st ed., Vol. 24, pp. 65–83). Elsevier Ltd. https://doi.org/10.1016/B978-0-12-811370-7.00004-8

Yu, T., Shiu, H., Lee, M., Chiueh, P., & Hou, C. (2016). Life cycle assessment of environmental impacts and energy demand for capacitive deionization technology. *Desalination*, *399*, 53–60. https://doi.org/10.1016/j.desal.2016.08.007

Zhang, C., Wang, X., Wang, H., Wu, X., & Shen, J. (2019). A positive-negative alternate adsorption effect for capacitive deionization in nano-porous carbon aerogel electrodes to enhance desalination capacity. *Desalination*, *458*, 45–53. https://doi.org/10.1016/j.desal.2019.01.023

Zhao, X., Wei, H., Zhao, H., Wang, Y., & Tang, N. (2020). Electrode materials for capacitive deionization: A review. *Journal of Electroanalytical Chemistry*, *873*, 114416. https://doi.org/https://doi.org/10.1016/j.jelechem.2020.114416